Applied Physics A (2019) 125:738
https://doi.org/10.1007/s00339-019-3036-4

Applied Physics A
Materials Science & Processing

Morphology stability of polymethylmethacrylate nanospheres formed in water–acetone dispersion medium

Ivan V. Nemtsev[1,2] · Olga V. Shabanova[4] · Nikolay P. Shestakov[2,3] · Alexander V. Cherepakhin[2,3] · Victor Ya. Zyryanov[1,2]

Received: 2 July 2019 / Accepted: 23 September 2019 / Published online: 3 October 2019

Abstract

The aim of this study is to develop a manufacturing technique of polymethylmethacrylate (PMMA) nanospheres to produce a more stable opal template. Water–acetone mixture was used as a dispersion medium to synthesize a PMMA opal structure. Morphology features, IR vibrational spectra and glass transition temperatures of the PMMA nanospheres formed in the water–acetone dispersion medium (nanospheres A) have been studied comparing with the same prepared in distilled water solution without acetone (nanospheres B). A dependence of a shrinkage degree of the nanoparticles on the acetone volume has been investigated. It has been revealed that under an electron beam action the shrinkage degree of the nanospheres A is in the range of 7–16% while the shrinkage of the nanospheres B is 18–25% at the same conditions. The nanospheres A are less flexible and soft as compared to the nanospheres B. Additionally, an ability of the PMMA nanoparticles fabricated in the water–acetone dispersion medium to form the ordered opal structures is demonstrated to be the similar to the nanospheres B.

1 Introduction

Poly(methyl methacrylate) (PMMA) is a well-known, amorphous, synthetic polymer [1–3]. PMMA is better known as an "organic glass" due to its high optical transparency. The polymer is comprehensively employed as a substitute for an inorganic glass for the reason that it shows high impact strength, lightweight, shatter-resistant, and exhibits favorable processing conditions [4]. An understanding of key properties of PMMA might facilitate enormously to a breakthrough in technological and laboratory manufacturing, chemical and physical transformation as well as expand a range of utilization of the polymer. The polymers, that bear specific chemical groups imparting new properties to materials for physical, chemical, biological, and pharmaceutical uses are called functional polymers [5]. PMMA is seemed to be the encouraging and attractive polymer for practical implementation in biomedical [6–8], sensor [9–11], electrochemical and conductive devices [12], optical [13, 14], analytical separation [15], solar cell technology [16–21], applications in nanotechnology [22–25] and other fields. For the biomedical applications, PMMA is the most promising polymer due to its non-toxicity, less cost, minimal inflammatory reactions with tissues, easy processability, and compatibility. Among the applications, it should be noted a drug delivery [26, 27], implant material [1], biological labeling [7, 28], therapeutics [29, 30], biodetection [30], bioimaging [30, 31]. In addition, PMMA has been one of the most commonly used polymers for microfluidics [6, 32]. Among the feasible optical application are temperature sensors and three-dimensional displays [10], extraordinary optical transmission [33], low-loss transmission [34], enhanced absorption [35, 36] and multi-functional and multi-responsive luminescence [37].

Electronic supplementary material The online version of this article (https://doi.org/10.1007/s00339-019-3036-4) contains supplementary material, which is available to authorized users.

✉ Ivan V. Nemtsev
ivan_nemtsev@mail.ru

[1] Federal Research Centre Krasnoyarsk Scientific Center of the Siberian Branch of the Russian Academy of Sciences, 50 Akademgorodok, 660036 Krasnoyarsk, Russia

[2] Kirensky Institute of Physics, Federal Research Centre Krasnoyarsk Scientific Center of the Siberian Branch of Russian Academy of Sciences, 50 Akademgorodok, 12 str, 660036 Krasnoyarsk, Russia

[3] Siberian Federal University, 79 Svobodny pr., 660041 Krasnoyarsk, Russia

[4] Special Designing and Technological Bureau "Nauka" Krasnoyarsk Scientific Center of the Siberian Branch of Russian Academy of Sciences, 50 Akademgorodok, 45 str., 660036 Krasnoyarsk, Russia

The organic glass may be also used for the manufacturing of micro- and nanosized nanospheres [38, 39]. To form the nanospheres, a technology based on distilled water medium is usually applied. A classical approach to synthesize the PMMA particles (soap-free emulsion polymerization) suggests using methyl methacrylate (MMA), distilled water and initiator only [40–42]. Such spheres might form ordered and even perfectly ordered 2D and 3D mesoporous structures (photonic crystal films, artificial opals) [43, 44]. It should be noted that there is a number of works devoted to the application of optical devices based on the photonic crystals (PhCs) [45–48]. Examples of the polymer-based PhCs are given in [49].

A particular case of the PhCs is an inverse opal (IO) [50–52]. IO macroporous structures have promising application in gas sensing [49], photocatalysis and even in cancer cell therapy. At present, the polymer templates are commonly used to fabricate the inverse opal. An essential part of the inverse opal manufacturing is a fabrication of the PMMA template [53], possessing a sufficient strength. Consequently, fusing of the PMMA nanospheres is required. There are many works both calculating and experimental on a thermal gravimetric analysis (TGA), differential thermal analysis (DTA), differential thermogravimetric (DTG) and differential scanning calorimetry (DSC) [4, 54–57]. Therefore, the understanding of the chemical and thermal properties such as an annealing temperature, tacticity, length of a polymer chain plays the crucial role in the strengthening of the PMMA template by the slightly fusing of the polymer particles.

The properties of the classical PMMA nanospheres are well studied. However, utilizing dispersion medium that is more complex, it is possible to modify [58] the polymerization technique and obtain the nanoparticles with the variable properties [59]. Current work is aimed at the study of the morphological stability of the PMMA nanospheres manufactured in the water–acetone dispersion medium.

2 Experimental

2.1 Materials and instrumentation

First, the PMMA nanospheres with a polydispersity less than 5% [48] were manufactured in the water dispersion medium to compare them with particles produced in the water–acetone dispersion medium. MMA (99.8%) from VitaReaktiv (Dzerginsk, Russia), nitrogen gas (99.6%) from TD Fakel (Krasnoyarsk, Russia) 2.2′-azobis(2-methylpropionamidine) dihydrochloride (97%) from Aldrich (St. Louis, Missouri, US) were used without further purification. In addition, distilled water and distilled acetone were used.

In situ disturbed total internal reflection measurements were carried out with the FTIR-spectrometer *FT-801* (Simex, Novosibirsk, Russia) to control a process of a synthesis. To ensure electrical conductivity, a magnetron sputter coater *K575XD* (Emitech, UK) was used to cover the surface of PMMA with a thin film. The morphological features of the samples was acquired with a high-resolution field emission scanning electron microscope (FE-SEM) *S-5500* (Hitachi, Japan) at an acceleration voltage of 3 kV. A scanning electron microscope SU3500 (Hitachi, Japan) was employed to visualize large areas of the PMMA opal films. A drying of the samples was performed using a laboratory oven with a digital thermometer *SIBLAB 30L* 350 °C (DION, Novosibirsk, Russia). Steady-state attenuated total reflectance spectroscopy was performed with the FTIR-spectrometer *Vertex 70* (Bruker, Germany). To investigate the glass transition temperature, the calorimetry experiments were performed using a premium differential scanning calorimeter *Phoenix 204 F-1* (NETZSCH, Germany).

2.2 Synthesis of poly (methyl methacrylate) nanospheres

Batches of the high-quality PMMA nanospheres with the very narrow polydispersity [48] were synthesized via a chain radical polymerization process of methyl methacrylate [50, 60]. Mean diameters in the batches were between 237 and 447 nm.

A size of the PMMA spheres produced using this method is highly dependent on a composition of a synthesis mixture and reaction temperature. Briefly, distilled water, methyl methacrylate and distilled acetone (in case of the water–acetone dispersion medium) were charged into a four-necked flat-bottomed cylinder (1 L in volume, made from stainless steel), equipped with a mechanical mixer, running a water-cooled reflux condenser and nitrogen bubbler. The mixture was then heated to 72.7–75 °C, whereupon 2,2′-azobis(2-methylpropionamidine) dihydrochloride was added as an azo initiator and the polymerization of MMA started.

Since a boiling point of acetone (56.1 °C) is much lower than that of water (100 °C) and MMA (101 °C), Sample 3 with a low MMA content boils at 75 °C. Therefore, we decreased the synthesis temperature down to 72.7 °C for all the nanospheres A. The works devoted to the synthesis temperature of polymers [61, 62] confirm that a slight temperature variation will not affect strongly the physical and chemical properties of the particles. In fact, only synthesis time of the nanospheres A became longer for 10–15 min in comparison with synthesis time of the nanospheres B. The measurements of variations in the reaction mixture temperature were made in the mode of dynamic observation.

Thus, to obtain the PMMA nanospheres B in the range of 360–370 nm (for example, as Sample 7), we used

150 ml of MMA, 570 ml of distilled water and 0.3 g of initiator diluted in 20 ml of distilled water. In that study, the emulsion temperature was kept at 75 °C and the mixer speed was fixed at 700 rpm [40–42, 48]. The polymerization procedure for mixing water and methyl methacrylate lasted for about 1.2 h. A concentration of the nanoparticles B in the water dispersion medium was estimated to be about 13 vol% ($6{\cdot}10^{15}$ nanoparticles per one liter). To achieve the PMMA nanospheres A with the minimal shrinkage (7%) and the average diameter 360 nm (Sample 6), we employed 100 ml of MMA, 550 ml of distilled water and 0.2 g of initiator diluted in 20 ml of distilled water. The emulsion temperature was kept at 72.7 °C and the mixer speed was fixed at 700 rpm. The polymerization procedure lasted for about 1.5 h. The concentration of the nanoparticles A in the water–acetone dispersion medium was estimated to be 23 vol%

In situ the FTIR-spectra of the emulsion every 5 min were recorded with the FT-801 to control at least two features of the polymerization. The first is to determine that the polymerization process finished (a sharp increase in temperature at deep reaction steps, because a hard gel effect is typical for the MMA polymerization [60, 63]). The second is to be sure that no monomer preserved in the dispersion [60].

The reaction mixture was maintained at the initial temperature for about 2 h under a vigorous mechanical stirring and then cooled to a room temperature over 2.5–3 h under a nitrogen purge. The resulting colloidal suspensions of the PMMA nanospheres were finally filtered through a filtering paper to remove a foam consisting from large agglomerates of the PMMA particles and then stored in glass bottles for later use. Table 1 summarizes the key parameters of the synthesis, dispersions and nanospheres such as a proportion of reagents, stirring speed, synthesis temperature, mean diameter of the particles before the shrinkage determined with SEM, degree of the shrinkage and average initial viscosity of the obtained dispersion media.

2.3 Self-assembly of opal-like colloidal structures

The colloidal structures based on the PMMA nanospheres were fabricated on cover glasses by a vertical deposition method [43]. The cover glass substrates were initially immersed into an ultrasonic cleaner filled with acetone for 10 min and then washed with distilled water to clean up the dirt on the surface. To estimate an aptitude of the particles to form the ordered structures, the degreased cover glass was instantly wetted vertically in the obtained non-diluted (13–23 vol% of the PMMA nanospheres) suspensions and placed on a horizontal surface in a Petri dish until the film was completely dry. Humidity in a laboratory box was constantly kept at 60% and temperature was constantly maintained at 23 °C. The purpose of this stage of the work was not to achieve the film with a single-crystal structure as in [46, 48, 64, 65], but an investigation of various ordering defects.

Rectangular plates of 3.5×7 mm were cut out of the glass. The samples were coated with the thin film of platinum in the magnetron to ensure electrical conductivity of the polymer particles and the cover glasses. To minimize a damage to the PMMA-opal films, coating modes were matched as follows: three cycles of 20 s with a given current of 10 milliamps. There also a gas argon was used to purge a chamber of the sputter coater.

2.4 Characterization

To improve an imaging quality, scanning modes of SEM as well as a sample preparation were selected individually for each experiment from the following ruminations: first, sample for SEM has to be electrically conductive. The PMMA particles are an insulator. Coating with the thin

Table 1 Parameter's table of the nanoparticles A and B

Sample number	MMA volume, ml	Water volume, ml	Acetone volume, ml	Stirring speed, rpm	Initiator mass, g	Synthesis temperature, °C	Mean diameter of particles before shrinkage, nm	Degree of shrinkage, %	Mean initial viscosity of a dispersion medium, $\times 10^{-4}$ Pa·s
1	50	670	0	700	0.1	75	237	24	8.73
2	50	640	30	700	0.1	75	254	14	8.37
3	50	600	70	700	0.1	72.7	286	12	7.92
4	100	620	0	700	0.2	75	303	18	8.52
5	100	590	30	700	0.2	75	330	9	8.18
6	100	550	70	700	0.2	72.7	358	7	7.73
7	150	570	0	700	0.3	75	369	25	8.32
8	150	540	30	700	0.3	75	409	16	7.99
9	150	500	70	700	0.3	72.7	447	14	7.55

metal film (for example, in magnetron with platinum) only aggravates the situation in case of the samples need to be certified: grains of the hot metal "spoils" the surface of the soft flexible polymer particles in the magnetron chamber. Then, the situation exacerbates when the particles in the SEM chamber are heated by an electron beam and slightly fused. Thus, it is hardly possible to estimate true particle sizes due to the shrinkage and charging up [63]. Therefore, the PMMA colloid was repeatedly diluted with distilled water, selecting the concentration [48, 63] of the PMMA particles in such a way as to obtain the single-layer island film on the substrate. An ideal option is to obtain the particles separated from each other on electrically conductive substrate (for example, on aluminum).

Second, the polymer particles under the action of the electron beam are able to shrink, melt and even explode in the chamber of the electron microscope. Therefore, in assessing the size, the individual PMMA particles were scanned at small magnifications at an accelerating voltage of 3 kV [60] and emission current of 10 μA but with a maximum resolution (2560 × 1920 px) and a slowest scan speed to minimize a noise and subsequently have a possibility of a digital image processing with a PC. Then, using an open source image editing program GIMP (GNU Image Manipulation Program), the sizes of the nanospheres were estimated [48].

To evaluate the shrinkage degree, one of the particles on the substrate was selected and captured by the above method. Then, the same particle was shot at the maximum possible high magnification to be still fully fitted in a computer monitor (k200–300x). Exposure time was 10 s, after that the particle did not shrink. Finally, the same particle was scanned for the third time at the initial magnification to be able to estimate its diameter after the shrinkage under the electronic probe. It should be noted, that the initial and the maximum magnification was the same in both cases to compare the particles of different samples. To estimate particle size distributions, we made a distribution histogram for each sample. The distribution histogram was built as follows: from figures at low magnification (× 15k), 100 particles were taken for each sample. The diameter of each particle was determined using GIMP. This program allows determining scale bars as well as particle sizes in pixels. Since we know the scale bar length in nanometres, the PMMA particle sizes in nanometres can be estimated using a pixel-to-nanometre ratio. The distribution histogram was built and the mean diameter was determined for each sample: $DSample1 = 237 \pm 3.39$ nm; $DSample2 = 254 \pm 3.34$ nm; $DSample3 = 286 \pm 6.62$ nm; etc. The particle-size dispersity is no more than 7 nm (3% deviation from the mean value). The method is described in more detail in [48].

3 Results

3.1 Electron microscopy

As we have already mentioned, the morphological features of the obtained particles were studied with the FE-SEM S-5500. The sizes of the particles, their sphericity, degree of the shrinkage as well as monodispersity were estimated.

Figure 1 demonstrates the shrinkage of the water–acetone samples 5, 3 and the water samples 4, 7 to compare. Here, we can see the shrinkage degree 25% of the nanoparticles B and only 7% of the nanoparticles A (Sample 5).

Summarizing the *Parameter's* Table 1, we can plot the following dependencies: the dependence of the shrinkage degree on the volume of acetone, mean diameter of the nanospheres on the volume of MMA, mean diameter of the nanospheres on the volume of acetone, mean diameter of the nanospheres on the initial viscosity of dispersion medium, as well as the degree of the shrinkage on the initial viscosity of dispersion medium, volume of MMA, volume of acetone and mean diameter of the particles.

There is no doubt the size of PMMA particle is known [61, 66–68] to depend on volume of MMA (Fig. 2a). Moreover, in our work, it was shown that the size of the PMMA particles depends on the volume of acetone (Fig. 2b); the more acetone volume, the larger particle size. The statement is valid for the acetone volume content in a dispersion medium for about 10%. No experiments at higher concentrations of acetone were performed.

All samples, regardless of the preparation conditions and the particle size, during the electron microscopic study showed approximately the same structures. Although, the samples made of nanospheres A (the particles from the dispersion media with acetone addition, Fig. 4d, k) packed only slightly better. Figure 4a–d demonstrates peculiar patterns of the particles found in the study.

Figure S2a, b show a cross-section of the PMMA film formed from the nanoparticles A (sample 3) and reveals no order in a bulk. The opal film is demonstrated to consist of about 12 layers. However, small quite ordered domains are observed in some places (Fig. 5) located, as a rule, at edges of drops. It should be noted that the nanoparticles A and B tend to form the similar ordered structures (Fig. 5b, Sample 1 and Fig. 5a, Sample 3).

3.2 ATR FTIR spectroscopy

All samples as well as the chemical reagents were also studied by the method of IR-spectroscopy. The IR-Fourier spectra were recorded using Vertex 70 with the use of an

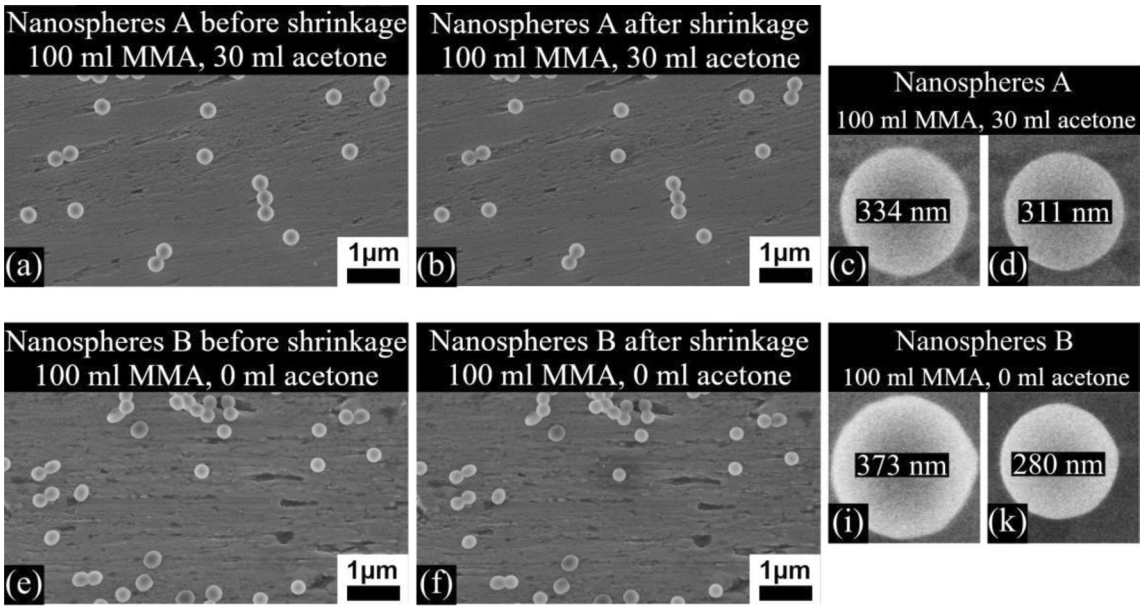

Fig. 1 Micrographs of nanospheres A of Sample 5 (top line) and nanospheres B of Sample 4 (bottom line). Photos (**a**, **b**, **e**, **f**) are taken at low magnification and (**c**, **d**, **i**, **k**) at high magnification; photos (**c**, **d**, **i**, **k**) are a comparison of particles before (left row) and after (right row) a shrinkage under an electron beam

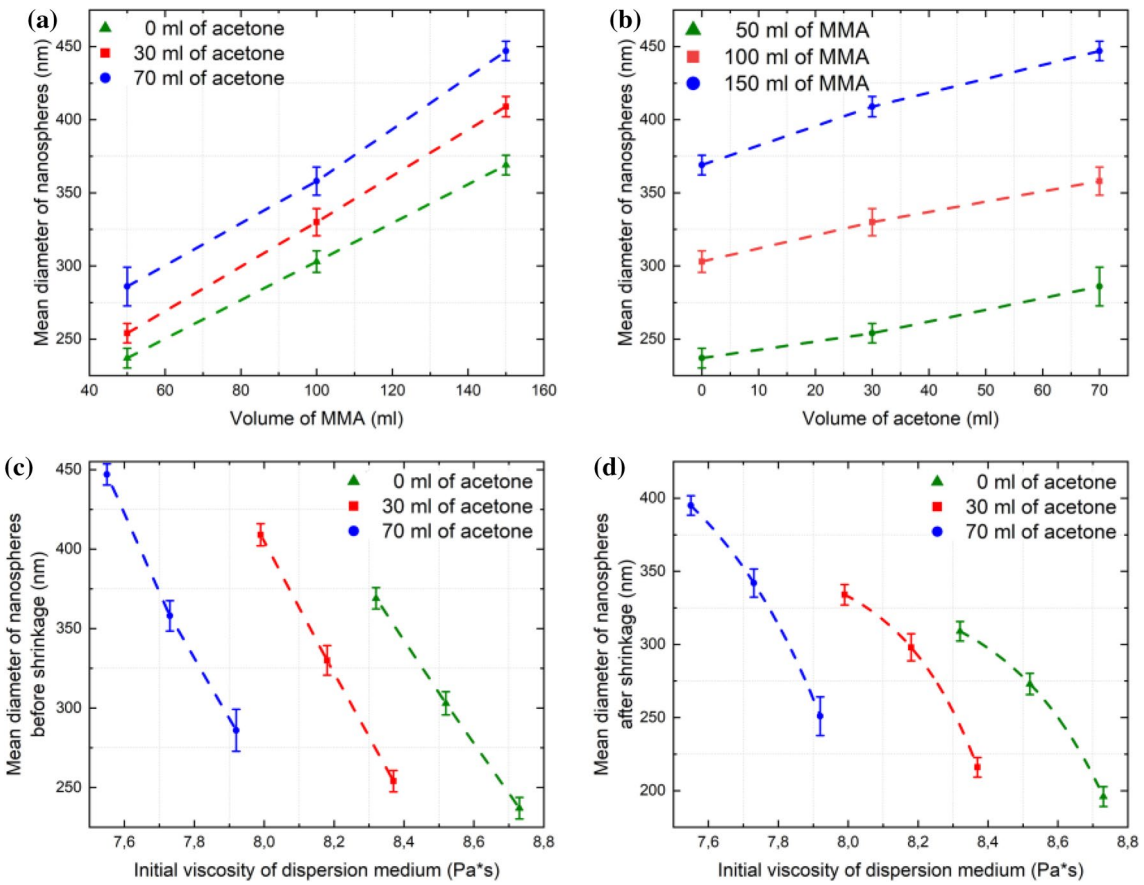

Fig. 2 Dependencies of a mean diameter of nanospheres: on volume of MMA (**a**), on volume of acetone (**b**). Dependences of a mean diameter of nanospheres on initial viscosity of a dispersion medium: before (**c**) and after (**d**) a shrinkage

attachment "HATR" (Pike, Madison, USA) with a Zinc Selenide ATR prism.

The ATR-spectra of distilled acetone, distilled water, pure MMA and the water (water–acetone) dispersions of the Samples 5, 6, 4 were obtained (Fig. 6). The ATR-spectra of the dried Samples 5, 6, 4 were also recorded.

4 Discussion

4.1 Electron microscopy discussion

The fact of less shrinkage of nanoparticles A might be caused by a capturing of a huge quantity of water during the synthesis in the case of the water samples in comparison to the water–acetone samples. In [61], authors write on obtaining of microspheres in a methanol-enriched aqueous medium. They expected that increasing methanol in the water content would result in a larger particle size. It has been suggested that this phenomenon is often observed in the dispersion polymerization where all ingredients are dissolved in medium such as methanol or ethanol. In the early stage of the dispersion polymerization, oligomers generated in homogeneous phase (i.e., solution polymerization occurs at this stage) grow until the critical chain length which cannot remain dissolved in the medium, and then precipitate to form primary particles. When the solvency of the medium is better, a smaller number of primary particles is generated since most oligomers exist in the medium, resulting in larger final particles. In this soap-free emulsion polymerization, all the ingredients are soluble in the methanol/water mixture; hence, initial reaction starts in solution phase to give surface active oligomeric species originated from the decomposition of initiator. As result, they conclude that the particle size tends to grow. However, the uniformity of size becomes poor.

We believe, that in our case, the longer polymer chain, which precipitates out of the solution and goes into the solid phase, captures more dispersion medium (water + acetone + MMA). Furthermore, with an increase of acetone amount, the solubility of MMA and its oligomers, which is captured by the polymer nanoparticle, increases. This leads to the fact that at the stage of the sol–gel effect, a large amount of polymer is formed inside the particle [69, 70]. Thus, by the time of the gel effect, the nanoparticles A contain more MMA and the growing oligomers inside themselves compared to the nanoparticles B. In addition, we believe, that if it is not considered influence of solid phase (polymer chains, oligomers, nanospheres) than in a nanoscale the viscosity of the dispersion medium changes insignificantly from the initiator addition to the gel effect. Besides, the DSC results demonstrate an increase of a glass temperature with an increase of MMA and acetone volumes (Table S2 in Online Resource). The maximum temperature has Sample 9 (126 °C). This assumption needs special investigation outside the scope of this article.

As we can see, Fig. 1a, b, reveals the very narrow polydispersity in contradistinction to [61, 71, 72]. However, in Fig. 1e, f the non-spherical particles are clearly visible. The spheres were damaged during the sample preparation. In case of the distilled water dispersion, the nanospheres are more flexible and soft in comparison with the water–acetone dispersion. The nanoparticles A (Samples 2, 3, 5, 6, 8, 9) are more rigid and solid that is confirmed with the SEM experimental study. They shrinked less (Fig. 1c, d) under the high magnification as well as they are also less damaged during the sample preparation (Fig. 1a, b).

Figure 2b demonstrates dependences of the mean diameter of the PMMA nanoparticles on the volume of acetone; the more the acetone volume, the lager the particle size are. We assume capturing of more numbers of MMA molecules during the polymerization process. That is why the PMMA nanospheres with the acetone addition are larger and more robust. However, not all dependencies of the shrinkage of the particles, both in aqueous and acetone dispersions, are linear. The shrinkage of the particles (Figs. 2d, 3a–d) can depend on a configuration of primary globules [70] forming the nanoparticles [73]. However, the configuration of the nanospheres, in its turn, depends on the parameters of dispersion medium. The comparable non-linear dependence of the physical parameters has been shown in [73]. Perhaps, this is due to a balance of polymer solubility [70, 74] and requires an additional research.

We found experimentally that the size of the nanoparticles is also affected the initial viscosity of the dispersion medium; the more the initial viscosity, the less the nanospheres are [75–77]. Furthermore, we believe that there is a dependence between the initial viscosity of the dispersion medium and the shrinkage (Fig. 3a). It is should be noticed that we cannot compare samples if volumes of MMA are different, because of different dissolubility of the dispersion media. Therefore, we have to separate all samples from Table 1 into three groups (1–2–3; 4–5–6; 7–8–9) or take into account an average value of the initial viscosity of the dispersion medium from each group (Figs. 2c, d, 3a).

For some engineering calculations, it is necessary to estimate a viscosity of a mixture of two or more components. In [78] reports that there are about seventeen mixing rules but the most used are Gambill, Grunberg-Nissan, Ratcliff's and Refutas methods [79]. To estimate the average viscosity of the dispersion media, we used the classic Grunberg-Nissan mixing rule for liquid mixture:

$$\ln \mu_{\text{mix}} = \sum x_i \ln \mu_i, \tag{1}$$

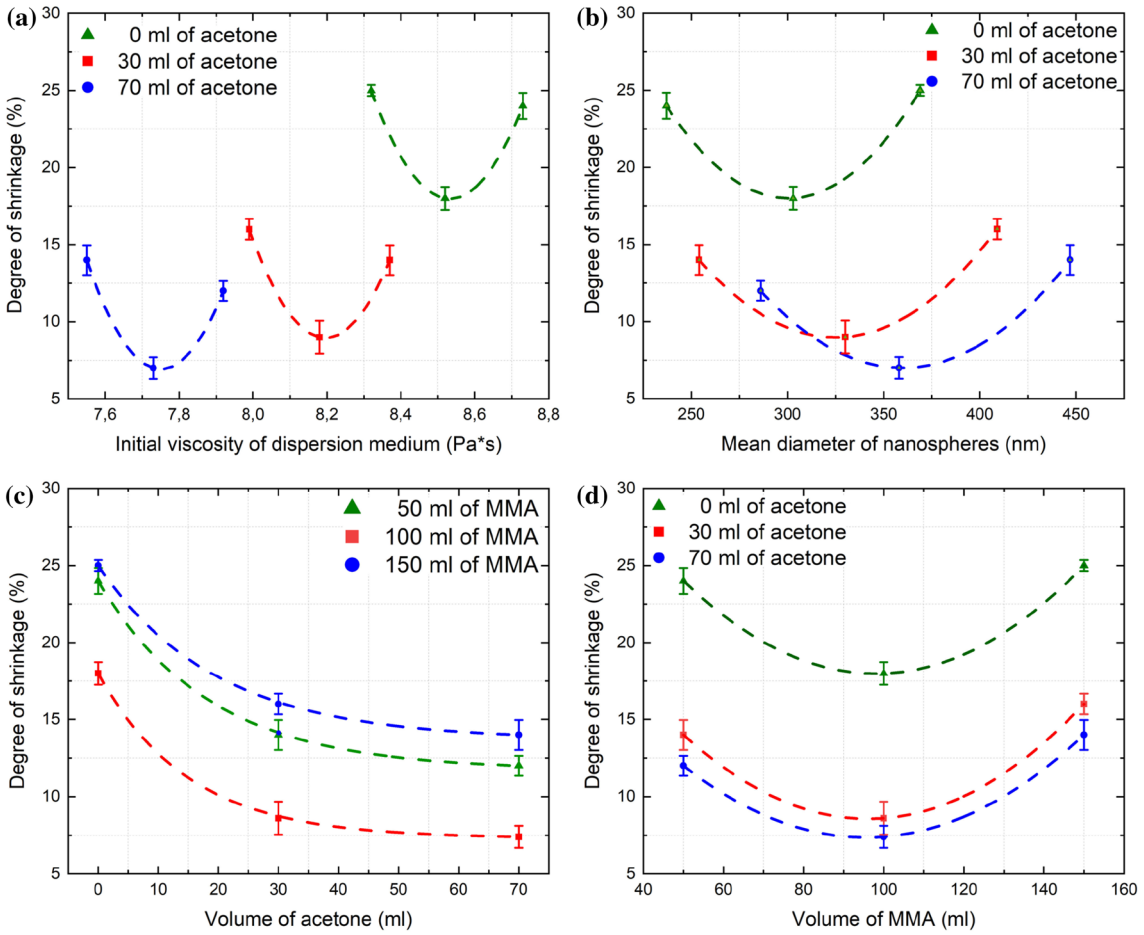

Fig. 3 Dependencies of a degree of a shrinkage: on initial viscosity of a dispersion medium (**a**), on a mean diameter of nanospheres before a shrinkage (**b**), on volume of acetone (**c**), on volume of MMA (**d**)

where μ_{mix} is the viscosity of the liquid mixture; x_i is the viscosity (equation) for fluid component i when flowing as a pure fluid, and μ_i is a mole fraction of component i in the liquid mixture.

We revealed that the mean diameter of the particles before the shrinkage depends linearly, but after the shrinkage depends exponentially on the initial viscosity of the dispersion medium (Fig. 2c, d).

It is well known that monodispersity and stability are required to form ordered closed-packed arrays, and diameters should not vary more than ≈ 5–8% [80]. However, in Fig. 4, small (for about 5–10 μm) ordered domains are formed, interleaving with regions (for about 5–20 μm), where a periodicity of the short-range order is observed. There is a number of defects such as a formation of cracks, domain boundaries, colloid vacancies, and others [81, 82] in manufacturing of opals. In its turn, the formation of the cracks might be associated with a liquid infiltration or drying [82]. A surface tension is revealed to play one of the crucial roles. Furthermore, it was determined experimentally that the more the order of the opal film the more defects it contains. The more the order, the deeper the cracks are. It is believed that the formation of the numerous microcracks is caused by the shrinkage of the particles and excessively fast sedimentation as well in case of the water–acetone dispersions, since the acetone solution evaporates much faster than the water solution. That is why the ordering decreases while sedimentation in films. This fact is especially noticeable for the large particles, which settle down faster.

4.2 ATR FTIR spectroscopy discussion

According to Bellamy and Nakanishi [83, 84], clear extremely strong MMA lines (Fig. 5a) such as 2955, 2931, 1728, 1639, 1439, 1325, 1301, 1199, 1163, 1021, 942 and 816 cm^{-1} were detected (Table S1 in Online Resource) only in the spectrum of the pure MMA but they are not found in the others. This suggests that the entire volume of MMA has reacted completely during the synthesis.

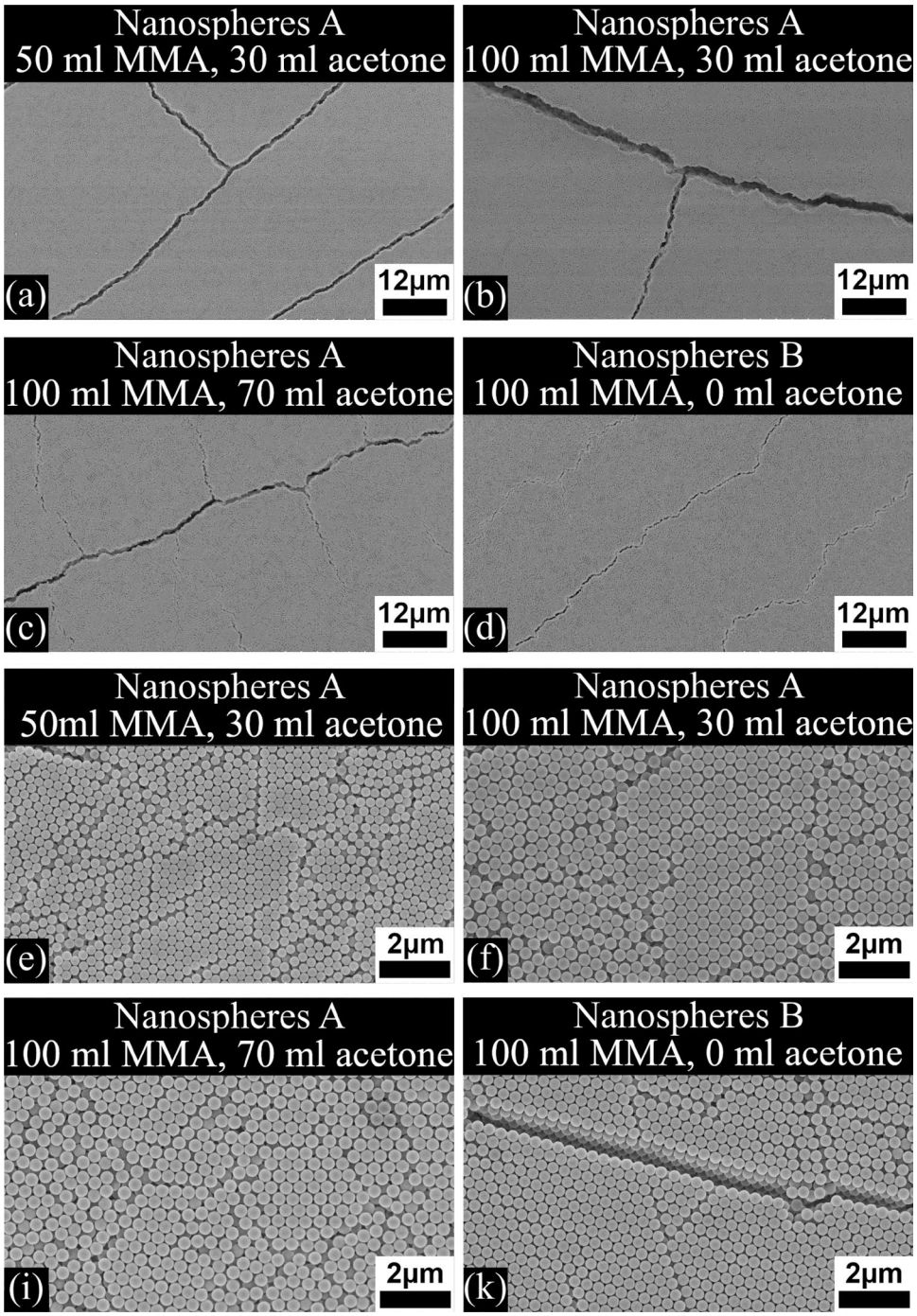

Fig. 4 SEM micrographs demonstrating a similar ability of nanospheres A and B to form ordered structures. Photos (**a**) Sample 2 (**b**) Sample 5 (**c**) Sample 6 (**d**) Sample 4 are taken at low magnification; photos (**e**) Sample 2 (**f**) Sample 5 (**i**) Sample 6 (**k**) Sample 4 are taken at high magnification

Due to the fact that the vibration bands of liquid water overlap the polymer peaks (at ~ 3430 and 1640 cm^{-1}), the dispersion media were dried at 80 °C for 3 h to evaporate the water from suspensions as well as the water contained in the PMMA particles. Furthermore, acetone peaks at 1716, 1422, 1362, 1222 and 1093 cm^{-1} have impact on identifying of vibration bands of PMMA.

After 3 h of drying, all three samples revealed no vibrational bands of acetone and water in the spectrum (Fig. 5c, d). Acetone and water were fully evaporated.

There is a well-known fact that PMMA can be synthesized as atactic (common, from a free radical polymerization), isotactic, or syndiotactic [2, 85, 86]. Stroupe's group was the first who reported the tacticity of PMMA in 1958 [87]. According to [2, 5, 88], the physical, chemical and mechanical properties of polymers with the different

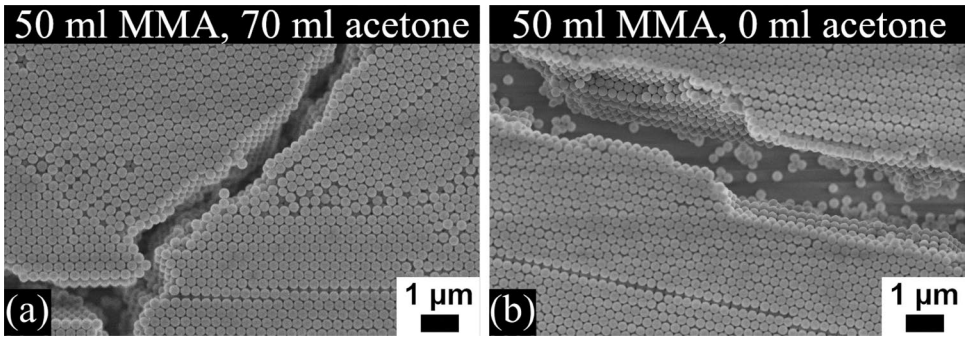

Fig. 5 SEM-micrographs of Sample 3 (**a**) and Sample 1 (**b**), demonstrating a similar order on edges of drops

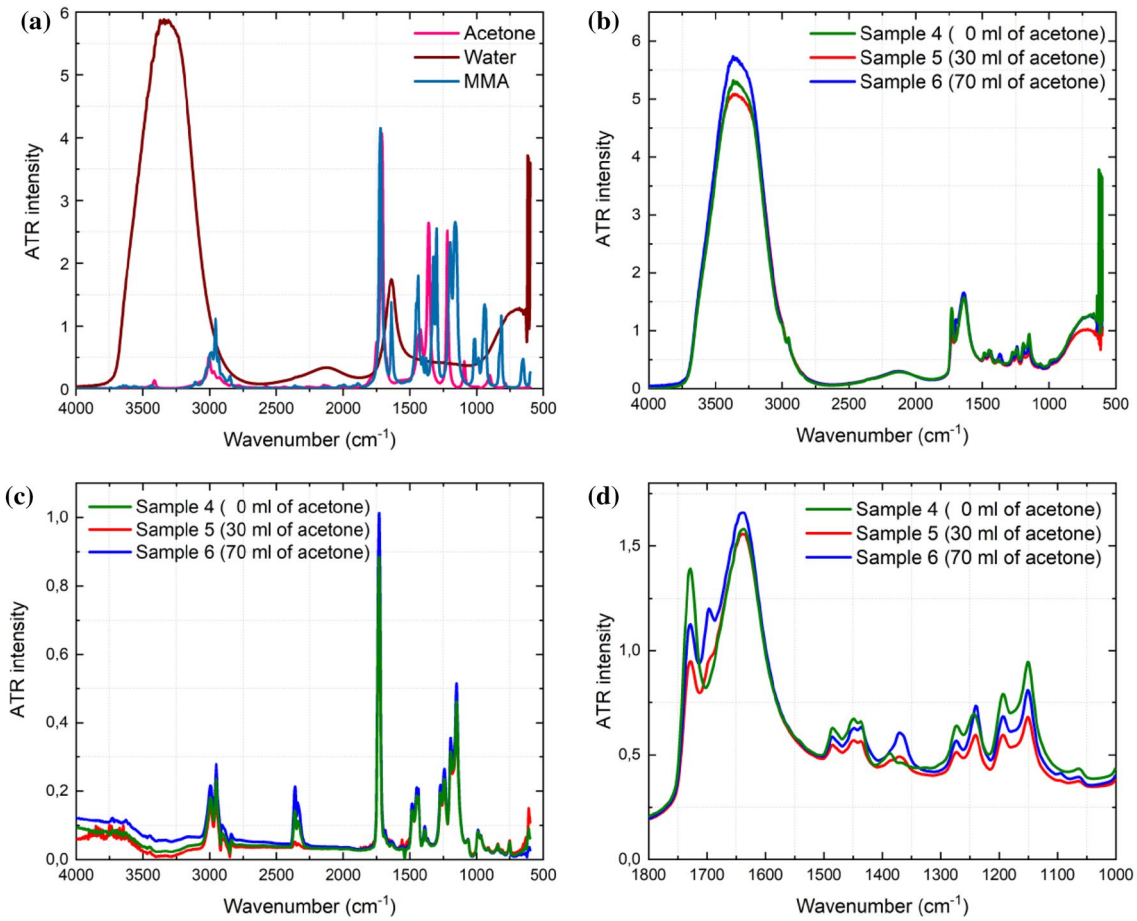

Fig. 6 ATR FTIR spectra of: **a** distilled acetone, distilled water, pure MMA; **b** distilled water (water–acetone) dispersions of Samples 5, 6, 4; **c** dried nanoparticles A and B (Samples 5, 6, 4); **d** a crop of **c**

stereoregularity are much different. Thus, the properties depended significantly on its tacticity are glass transitions and melting temperatures [86], viscosity, density, impact strength [1], processing conditions [89], crystallinity [90], elasticity [4], and many more.

The IR spectra of the dried at room temperature samples reviled that PMMA produced and discussing in this work is syndiotactic. This fact confirms by the infrared spectroscopy represented in Fig. 6d. According to [91], there are five peaks associated with an ester group of the syndiotactic PMMA. Moreover, relying on the DSC results, we can conclude that the tacticity of PMMA nanospheres corresponds to syndiotactic (Table S2, Fig. S1 in Online Resource).

In addition, the other peaks from Table S2 correspond to syndiotactic PMMA. All vibrational bands of this spectra were found in a good agreement with the literature values [13, 92–94] as well as with Bellamy and Nakanishi [83, 84].

5 Conclusions

To increase the morphological stability of an opal template structure, the PMMA nanoparticles have been fabricated using the emulsion polymerization in the water–acetone dispersion medium. The influence of the acetone content on the morphological features of the PMMA spheres and modification of mesoporous films as well as on their optical, physical and chemical properties have been studied using SEM, ATR FTIR and DSC methods. The degree of the shrinkage of the polymer nanospheres B is shown to be higher in contrast with the nanospheres A and amounted to 18–25% and 7–16%, respectively. It has been revealed that the PMMA particles became stronger, harder and more toughness when some quantity of acetone is added. It has been shown that the PMMA nanoparticles synthesized in the distilled water dispersion medium tends to form a bit more ordered photonic crystal films, because in case of the water–acetone dispersion, a liquid evaporates faster, so the spheres do not have enough time to keep within the ordered opal structure. There were experimentally found the complex dependencies of the particle shrinkage on various factors. These observed dependencies are of considerable interest and require an additional research.

The ATR FTIR spectroscopy has revealed that the PMMA nanospheres contain considerable amount of water which evaporation leads to the shrinkage of the spheres. Besides, the tacticity of PMMA manufactured in this study has been investigated and demonstrated that the PMMA nanospheres are syndiotactic. In addition, the glass transition temperature has been determined. It was 121–126 °C. Such temperature is found out to correspond the syndiotactic type of PMMA.

There has been experimentally established that the most optimal ratio of chemical reagents to obtain a stable PMMA template is as follows: 100 ml of MMA, 550 ml of distilled water, 70 ml of distilled acetone and 0.2 g of initiator.

The results can be helpful for the applications of the considered PMMA nanospheres as well as the obtained opal template structures in the fields of therapeutics and biological labeling, biodetection and bioimaging, solar cell technology, temperature sensors and three-dimensional displays, multi-functional luminescence, battery electrolytes, and other nanotechnology applications.

6 Author contributions.

Ivan V. Nemtsev initiated this study, performed the electron microscopy investigations as well as made the interpretation of obtained data; Olga V. Shabanova developed technology and produced PMMA colloids and fabricated the opal template structures; Nikolay P. Shestakov carried out the ATR FTIR measurements and took part in their discussion; Alexander V. Cherepakhin implemented the DSC experiments and contributed in their consideration; Victor Ya. Zyryanov supervised the study. All authors wrote and reviewed the manuscript.

Acknowledgements We are grateful to the Center of collective use of FRC KSC SB RAS for the provided equipment.

Compliance with ethical standards

Conflict of interest The authors declare that they have no conflict of interests.

References

1. U. Ali, K.J.B.A. Karim, N.A. Buang, Polym. Rev. **55**, 678 (2015)
2. F.A. Behbahani, S.M. Vaez Allaei, H.G. Motlagh, H. Eslami, V.A. Harmandaris, Soft Matter **51**, 7518 (2018)
3. R. Goseki and T. Ishizone, in Encycl. Polym. Nanomater. (Springer Berlin Heidelberg, Berlin, Heidelberg, 2015), pp. 1702–1710
4. N. Berrahou, A. Mokaddem, B. Doumi, S. Hiadsi, N. Beldjoudi, A. Boutaous, Polym. Bull. **73**, 3007 (2016)
5. F. Adams, P. Pahl, B. Rieger, Chem. A Eur. J. **24**, 509 (2018)
6. Y. Chen, L. Zhang, G. Chen, Electrophoresis **29**, 1801 (2008)
7. C. Bouzigues, T. Gacoin, A. Alexandrou, ACS Nano **5**, 8488 (2011)
8. S. Lazzari, D. Moscatelli, F. Codari, M. Salmona, M. Morbidelli, L. Diomede, J. Nanoparticle Res. **14**, 920 (2012)
9. W.-K. Kuo, H.-P. Weng, J.-J. Hsu, H. Yu, Appl. Sci. **6**, 67 (2016)
10. S.Y. Lin, J.G. Fleming, D.L. Hetherington, B.K. Smith, R. Biswas, K.M. Ho, M.M. Sigalas, W. Zubrzycki, S.R. Kurtz, J. Bur, Nature **394**, 251 (1998)
11. A. Bearzotti, A. MacAgnano, S. Pantalei, E. Zampetti, I. Venditti, I. Fratoddi, M. Vittoria Russo, J. Phys. Condens. Matter **20**, 474207 (2008)
12. H. Hashim, N.I. Adam, N.H.M. Zaki, Z.S. Mahmud, C.M.S. Said, M.Z.A. Yahya, A.M.M. Ali, CSSR 2010–2010 Int. Conf. Sci. Soc. Res. (Kuala Lumpur, Malaysia 2010), pp. 485–488
13. K. Gipson, K. Stevens, P. Brown, J. Ballato, J. Spectrosc. **2015**, 9 (2015)
14. I. Venditti, Materials (Basel) **10**, 97 (2017)
15. G. Bin Lee, S.H. Chen, G.R. Huang, W.C. Sung, Y.H. Lin, Sensors Actuators. B Chem. **75**, 142 (2001)
16. L. Xu, C. Aumaitre, Y. Kervella, G. Lapertot, C. Rodríguez-Seco, E. Palomares, R. Demadrille, P. Reiss, Adv. Funct. Mater. **10**, 97 (2018)
17. X. Huang, S. Han, W. Huang, X. Liu, Chem. Soc. Rev. **42**, 173 (2013)
18. H.-Q. Wang, M. Batentschuk, A. Osvet, L. Pinna, C.J. Brabec, Adv. Mater. **23**, 2675 (2011)

19. B. Shao, Z. Yang, Y. Wang, J. Li, J. Yang, J. Qiu, Z. Song, A.C.S. Appl, Mater. Interfaces **7**, 25211 (2015)
20. D. Bi, C. Yi, J. Luo, J.D. Décoppet, F. Zhang, S.M. Zakeeruddin, X. Li, A. Hagfeldt, M. Grätzel, Nat. Energy **1**, 16142 (2016)
21. M.K. Assadi, H. Hanaei, N.M. Mohamed, R. Saidur, S. Bakhoda, R. Bashiri, M. Moayedfar, Appl. Phys. A Mater. Sci. Process. **122**, 821 (2016)
22. M. Perween, D.B. Parmar, G.R. Bhadu, D.N. Srivastava, Analyst **139**, 5919 (2014)
23. X. Wang, P. Wang, Y. Jiang, Q. Su, J. Zheng, Compos. Sci. Technol. **104**, 1 (2014)
24. J.H. Sung, H.S. Kim, H.J. Jin, H.J. Choi, I.J. Chin, Macromolecules **37**, 9899 (2004)
25. L. Zhang, Y. Ren, S. Peng, D. Guo, S. Wen, J. Luo, G. Xie, Nanoscale **11**, 8237 (2019)
26. A. Bettencourt, A.J. Almeida, J. Microencapsul. **29**, 353 (2012)
27. I. Venditti, J. King Saud Univ. Sci. **31**, 398 (2019)
28. Q. Liu, T. Yang, W. Feng, F. Li, J. Am. Chem. Soc. **134**, 5390 (2012)
29. Zhang Li.X, Zhao D, Nano Today **8**, 643 (2013)
30. Y. Liu, D. Tu, H. Zhu, X. Chen, Chem. Soc. Rev. **42**, 6924 (2013)
31. M. Nyk, R. Kumar, T.Y. Ohulchanskyy, E.J. Bergey, P.N. Prasad, Nano Lett. **8**, 3834 (2008)
32. J. Li, D. Chen, G. Chen, Anal. Lett. **38**, 1127 (2005)
33. O. Glushko, R. Brunner, R. Meisels, S. Kalchmair, G. Strasser, Opt. Express **20**, 17174 (2012)
34. M.D. Nielsen, C. Jacobsen, N.A. Mortensen, J.R. Folkenberg, H.R. Simonsen, Opt. Express **12**, 1372 (2004)
35. L. Zeng, P. Bermel, Y. Yi, B.A. Alamariu, K.A. Broderick, J. Liu, C. Hong, X. Duan, J. Joannopoulos, L.C. Kimerling, Appl. Phys. Lett. **93**, 221105 (2008)
36. S. Nishimura, N. Abrams, B.A. Lewis, L.I. Halaoui, T.E. Mallouk, K.D. Benkstein, Jao van de Lagemaat, and A. J. Frank **125**, 6306 (2003)
37. H. Wang, X. Gu, R. Hu, J.W.Y. Lam, D. Zhang, B.Z. Tang, J. van de Lagemaat, A.J. Frank, Y.-P. Li, Y.-G. Ma, H.-B. Sun, D. Zhang, D. Wiersma, G.A. Ozin, Chem. Sci. **7**, 5692 (2016)
38. T.R. Paxton, J. Colloid Interface Sci. **31**, 19 (1969)
39. Z.Z. Gu, Y.H. Yu, H. Zhang, H. Chen, Z. Lu, A. Fujishima, O. Sato, Appl. Phys. A Mater. Sci. Process. **81**, 47 (2005)
40. D. Zou, J.J. Aklonis, R. Salovey, J. Polym. Sci. Part A-1 Polym. Chem. **30**, 2443 (1992)
41. J.C. Ruiz-Morales, J. Canales-Vázquez, J. Peña-Martínez, D. Marrero-López, J.T.S. Irvine, P. Núñez, J. Mater. Chem. **16**, 540 (2006)
42. P.J. Lou, W.F. Cheng, Y.C. Chung, C.Y. Cheng, L.H. Chiu, T.H. Young, J. Biomed. Mater. Res. Part A **88A**, 849 (2008)
43. G.I.N. Waterhouse, W.T. Chen, A. Chan, D. Sun-Waterhouse, ACS Omega **3**, 9658 (2018)
44. Z.Z. Gu, A. Fujishima, O. Sato, Chem. Mater. **14**, 760 (2002)
45. J. Liao, Z. Yang, H. Wu, D. Yan, J. Qiu, Z. Song, Y. Yang, D. Zhou, Z. Yin, J. Mater. Chem. C **1**, 6541 (2013)
46. T. Xia, W. Luo, F. Hu, W. Qiu, Z. Zhang, Y. Lin, X.Y. Liu, A.C.S. Appl, Mater. Interfaces **9**, 22037 (2017)
47. Y. Wang, S. Dou, L. Shang, P. Zhang, X. Yan, K. Zhang, J. Zhao, Y. Li, Crystals **8**, 453 (2018)
48. I.V. Nemtsev, I.A. Tambasov, A.A. Ivanenko, V.Y. Zyryanov, Photonics Nanostructures Fundam. Appl. **28**, 37 (2018)
49. C.S. Lee, Z. Dai, S.Y. Jeong, C.H. Kwak, B.Y. Kim, D.H. Kim, H.W. Jang, J.S. Park, J.H. Lee, Chem. A Eur. J. **22**, 7102 (2016)
50. N. Matsuura, S. Yang, P. Sun, H.E. Ruda, Appl. Phys. A Mater. Sci. Process. **81**, 379 (2005)
51. E. Armstrong, C. O'Dwyer, J. Mater. Chem. C **3**, 6109 (2015)
52. P.P. Shetty, R. Zhang, J.P. Angle, P.V. Braun, J.A. Krogstad, Chem. Mater. **30**, 1648 (2018)
53. K. Kamitani, T. Hyodo, Y. Shimizu, M. Egashira, J. Mater. Sci. **45**, 3602 (2010)
54. C.G. Otoni, M.V. Lorevice, M.R.D. Moura, L.H.C. Mattoso, Carbohydr. Polym. **185**, 105 (2018)
55. M.E. Diken, S. Doğan, Y. Turhan, M. Doğan, Int. J. Polym. Mater. Polym. Biomater. **18**, 54 (2018)
56. N.A. Rangel-Vázquez, J.R. Campos-Cruz, J.E. Jaime-Leal, R. Rangel-Vázquez, in Hybrid Polym. Compos. Mater. Process., (Matthew Deans, Cambridge, 2017), pp. 307–330
57. A. Alonso Ipiña, M. Lázaro Urrutia, D. Lázaro Urrutia, D. Alvear Portilla, J. Phys. Conf. Ser. **1107**, 032011 (2018)
58. R. D'Amato, I. Venditti, M.V. Russo, M. Falconieri, J. Appl. Polym. Sci. **102**, 4493 (2006)
59. R. De Angelis, I. Venditti, I. Fratoddi, F. De Matteis, P. Prosposito, I. Cacciotti, L. D'Amico, F. Nanni, A. Yadav, M. Casalboni, M.V. Russo, J. Colloid Interface Sci. **414**, 24 (2014)
60. O.V. Shabanova, M.A. Korshunov, I.V. Nemtsev, A.V. Shabanov, Nanotechnol. Russ. **11**, 633 (2016)
61. S.E. Shim, E. Al, K. Kim, S. Oh, S. Choe, E. Al, Macromol. Res. **12**, 240 (2004)
62. B. Liu, Y. Wang, M. Zhang, H. Zhang, Polymers (Basel). **8**, 55 (2016)
63. I. Nemtsev, Vestn. SibSAU **1**, 126 (2012)
64. J.-H. Yoo, H.-J. Kwon, D. Paeng, J. Yeo, S. Elhadj, C.P. Grigoropoulos, Nanotechnology **27**, 145604 (2016)
65. Y. Huang, J. Zhou, B. Su, L. Shi, J. Wang, S. Chen, L. Wang, J. Zi, Y. Song, L. Jiang, J. Am. Chem. Soc. **134**, 17053 (2012)
66. Q. Ye, Z. Zhang, H. Jia, W. He, X. Ge, J. Colloid Interface Sci. **253**, 279 (2002)
67. T.Y. Kwon, J.Y. Ha, J.N. Chun, J.S. Son, K.H. Kim, Biomed. Res. Int. **2014**, 6 (2014)
68. M.J. Ballard, D.H. Napper, R.G. Gilbert, J. Polym. Sci. Polym. Chem. Ed. **22**, 3225 (1984)
69. K.E.J. Barrett, *in John Wiley Sons Ltd* (Wiley, New York, 1974), p. 322
70. R.M. Fitch, C.H. Tsai, in Polym. Colloids (1971), pp. 73–102.
71. A.L. Tasker, J.P. Hitchcock, L. He, E.A. Baxter, S. Biggs, O.J. Cayre, J. Colloid Interface Sci. **484**, 10 (2016)
72. J. Aubry, F. Ganachaud, J.P.C. Addad, B. Cabane, Langmuir **25**, 1970 (2009)
73. A.V. Shabanov, O.V. Shabanova, M.A. Korshunov, Colloid J. **76**, 113 (2014)
74. Z. Li, H. Liu, L. Zeng, H. Liu, Y. Wang, J. Mater. Sci. **51**, 9005 (2016)
75. K.E.J. Barrett, H.R. Thomas, J. Polym. Sci. Part A Polym. Chem. **7**, 2621 (1969)
76. K.F. Silveira, I.V.P. Yoshida, S.P. Nunes, Polymer (Guildf). **36**, 1425 (1995)
77. R.A.A. Tahrin, N.S. Azma, S. Kassim, N.A. Harun, in AIP Conference Proceedings (American Institute of Physics, 2017), p. 1885.
78. G. Centeno, G. Sánchez-Reyna, J. Ancheyta, J.A.D. Muñoz, N. Cardona, Fuel **90**, 3561 (2011)
79. M. Hoang, *Tuning of Viscosity and Density of Non-Newtonian Fluids through Mixing Process Using Multimodal Sensors, Sensor Fusion and Models* (Porsgrunn, Norway, 2016), p. 31
80. A. Stein, Microporous Mesoporous Mater. **44–45**, 227 (2001)
81. J. Gutmann, J. Posdziech, M. Peters, L. Steidl, R. Zentel, H. Zappe, and J. C. Goldschmidt, in Proceedings of SPIE (2012), p. 8438.
82. B. Hatton, L. Mishchenko, S. Davis, K.H. Sandhage, J. Aizenberg, Proc. Natl. Acad. Sci. **107**, 10354 (2010)
83. K. Nakanishi, J. Pharm. Sci. **52**, 716 (1963)
84. L.J. Bellamy, J. Chem. Educ. **36**, 366 (1963)
85. J. Sharma, X. Zhang, T. Sarker, X. Yan, L. Washburn, H. Qu, Z. Guo, A. Kucknoor, S. Wei, Polymer (Guildf). **55**, 3261 (2014)

86. D.W. van Krevelen, K. te Nijenhuis, Properties of Polymers, Fourth Edition: Their Correlation with Chemical Structure; Their Numerical Estimation and Prediction from Additive Group Contributions (2009), pp. 167–172
87. T.G. Fox, B.S. Garrett, W.E. Goode, S. Gratch, J.F. Kincaid, A. Spell, J.D. Stroupe, J. Am. Chem. Soc. **80**, 1768 (1958)
88. K.C. Jha, H. Zhu, A. Dhinojwala, M. Tsige, Langmuir **30**, 12775 (2014)
89. M.M. Demir, M. Memesa, P. Castignolles, G. Wegner, Macromol. Rapid Commun. **27**, 763 (2006)
90. P.N. Tzounis, D.V. Argyropoulou, S.D. Anogiannakis, D.N. Theodorou, Macromolecules **51**, 6878 (2018)
91. S. Havriliak, N. Roman, Polymer (Guildf). **7**, 387 (1966)
92. H.A. Willis, V.J.I. Zichy, P.J. Hendra, Polymer (Guildf). **10**, 737 (1969)
93. S.K. Dirlikov, J.L. Koenig, Appl. Spectrosc. **33**, 555 (1979)
94. S.N. Tripathi, P. Saini, D. Gupta, V. Choudhary, J. Mater. Sci. **48**, 6223 (2013)